Murray, in *Mars*, H. H. Kieffer *et al*., Eds. (Univ. of Arizona Press, Tucson, AZ, 1992), chap. 23.
12. D. A. Paige, K. D. Keegan, *J. Geophys. Res.* **99**, 25993 (1994).
13. M. D. Hofstadter, B. C. Murray, *Icarus* **84**, 352 (1990).
14. W. V. Boynton *et al*., *Science* **297**, 81 (2002).
15. Reviews of martian conditions discuss polar caps (*46*), water in the atmosphere (*47*), and annual polar caps (*48*).
16. TES albedo measurements were used because the THEMIS Visible Imaging Subsystem (VIS) images are not currently radiometrically calibrated.
17. The strip of seasonal CO_2 that lies between unit I and unit D narrows in size as summer progresses.
18. The default calibration yielded brightness temperatures for unit C below the saturation temperature of CO_2 at the surface elevation. The radiance levels for the entire THEMIS strip were adjusted to bring the brightness temperature of unit C to 144 K, as expected from extensive TES observations.
19. Bolometer observations were used instead of the spectrometer observations because of better spatial and temporal coverage.
20. MOC imaging of this region during early spring showed only unit D as not completely covered by CO_2.
21. A sol is one full martian day, 24.6 hours.
22. The properties of pure solid H_2O at 165 K are thermal conductivity k = 3.42 J m^{-1} $K^{-1/2}$ s^{-1}, density ρ = 928 kg m^{-3}, and specific heat C_p = 1310 J kg^{-1} K^{-1}, yielding a thermal inertia $(k\rho C_p)^{1/2}$ of 2044 J m^{-2} K^{-1} $s^{-1/2}$.
23. The models solve the subsurface thermal diffusion equation with a boundary condition of insolation and a one-layer atmosphere by using the Delta-Eddington radiative approximation. A typical martian dust opacity of 0.2 is used, with CO_2 frost condensation if the temperature falls below the saturation point for the current local atmospheric pressure. The Viking lander seasonal pressure variation is used (*49*). Models were run for 4 years to attain annual convergence, adjusting the solid CO_2 budget to disappear at the observed date for each area, then for another 80 martian days (sols) with 1-sol spacing.
24. A nominal TES footprint is either 3 km by 5 km or 3 km by 9 km, depending on whether TES is operating in 10 cm^{-1} or 5 cm^{-1} mode, respectively.
25. M. T. Mellon, B. M. Jakosky, H. H. Kieffer, P. R. Christensen, *Icarus* **148**, 437 (2000).
26. Typical thermal inertia values for dust and rock are 50 J m^{-2} K^{-1} $s^{-1/2}$ and 1260 J m^{-2} K^{-1} $s^{-1/2}$, respectively.
27. At the observed maximum temperature (200 K at L_S = 315°), unit I will be sublimating into the atmosphere, and this will somewhat suppress the temperatures. Although the sublimation rate is difficult to constrain without knowledge of the lowest boundary layer conditions, an estimate can be made by assuming that the column water vapor typical of late summer conditions, about 10 precipital micrometers (*35*, *36*), is replenished every martian day. This corresponds to a sublimation power of 0.3 W m^{-2}, or about 0.2% of the average absorbed solar flux; the surface temperature is lowered by less than 0.2 K.
28. H_2O grains in the atmosphere probably nucleate on dust grains. H_2O and dust probably accumulate with the south polar seasonal frost, both with mixing ratios to CO_2 of about 10^{-4} (*34*).
29. See figure 17 in (*30*).
30. H. Kieffer, T. Titus, K. Mullins, P. Christensen, *J. Geophys. Res.* **105**, 9653 (2000).
31. See Mellon 1993 (*43*), 1995 (*44*), and 1997 (*45*) for a detailed discussion.
32. Based on modeling of the albedo of dust-ice mixtures for the north polar cap, the increment of albedo from 0.23 to 0.30 for the S/I transition indicates that $f \times (r_H/r_d)^3 \sim 3$, where r_H is the ice grain radius, r_d the dust grain radius, and f the dust fraction. Thus, assuming that the dust is captured atmospheric dust (with a radius of ~2 μm), dust fractions of 0.1 and 0.0001 would imply ice grain radii of 8 to 80 μm.
33. K. E. Herkenhoff, *USGS Misc. Inv. Series Map Series I-2686* (2001).
34. E. S. Barker, R. A. Schorn, A. Woszczyk, R. G. Tull, S. J. Little, *Science* **170**, 1308 (1970).
35. B. Jakosky, J. Farmer, *J. Geophys. Res.* **87**, 2999 (1982).
36. M. D. Smith, J. L. Bandfield, M. I. Richardson, P. R. Christensen, paper presented at the annual meeting of the Division of Planetary Scientists, Birmingham, AL, 6 to 11 October 2002.
37. B. M. Jakosky, R. M. Haberle, *J. Geophys. Res.* **95**, 1359 (1990).
38. M. C. Malin, M. A. Caplinger, S. D. Davis, *Science* **294**, 2146 (2001).
39. CO_2 would quickly sublime if it were buried under a warmer material, and nothing with connection to the atmosphere can be colder than solid CO_2.
40. C. B. Farmer, P. E. Doms, *J. Geophys. Res.* **84**, 2881 (1979).
41. A. P. Zent, F. P. Fanale, J. R. Salvail, S. E. Postawko, *Icarus* **67**, 19 (1986).
42. D. A. Paige, *Nature* **356**, 43 (1992).
43. M. T. Mellon, B. M. Jakosky, *J. Geophys. Res.* **98**, 3345 (1993).
44. _____, *J. Geophys. Res.* **100**, 11781 (1995).
45. _____, S. W. Postawko, *J. Geophys. Res.* **102**, 19357 (1997).
46. F. Forget, in *Solar System Ices*, B. Schmitt *et al*., Eds. (Kluwer Academic, Dordrecht, Netherlands, 1998), pp. 447–510.
47. B. M. Jakosky, R. M. Haberle, in *Mars*, H. H. Kieffer *et al*., Eds. (Univ. of Arizona Press, Tucson, AZ, 1992), chap. 28.
48. P. B. James, H. H. Kieffer, D. A. Paige, in *Mars*, H. H. Kieffer *et al*., Eds. (Univ. of Arizona Press, Tucson, AZ, 1992), chap. 27.
49. J. E. Tillman, N. C. Johnson, P. Gettorp, D. B. Percival, *J. Geophys. Res.* **98**, 10963 (1993).
50. We acknowledge the extensive effort by J. Bell III and T. McConnochie to achieve relative calibration of THEMIS VIS images, including V00910003.

14 November 2002; accepted 25 November 2002
Published online 5 December 2002;
10.1126/science.1080497
Include this information when citing this paper.

A Sublimation Model for Martian South Polar Ice Features

Shane Byrne* and Andrew P. Ingersoll

In their pioneering work, Leighton and Murray argued that the Mars atmosphere, which at present is 95% carbon dioxide, is controlled by vapor equilibrium with a much larger polar reservoir of solid carbon dioxide. Here we argue that the polar reservoir is small and cannot function as a long-term buffer to the more massive atmosphere. Our work is based on modeling of the circular depressions commonly found on the south polar cap. We argue that a carbon dioxide ice layer about 8 meters thick is being etched away to reveal water ice underneath. This is consistent with thermal infrared data from the Mars Odyssey mission.

In 1966, Leighton and Murray (*1*) proposed that the martian polar caps constitute a permanent reservoir of CO_2 that is much larger than the atmospheric reservoir and whose vapor pressure determines the average atmospheric pressure at the surface on Mars. The north pole was favored to have more CO_2 (*2*) because its lower elevation allows CO_2 ice to equilibrate with the atmosphere at a higher temperature and pressure than in the south. Viking observations showed just the opposite: The north polar ice cap loses its seasonal covering of CO_2 each year, although the south polar ice cap does not (*3*, *4*). The north residual cap (the part that survives the summer) is therefore H_2O ice (*5*), which is less volatile than CO_2 ice. The survival of CO_2 ice in the south might be due to the lower concentration of dust, as compared with that of the north cap, and consequent high albedo, which allows it to absorb less sunlight (*6*, *7*).

However, there are other problems with the Leighton and Murray model. First, the rapid springtime retreat of the seasonal ice implies a rate of mass loss that is incompatible with the long-term survival of CO_2 ice (*8*, *9*). Second, in 1969 there was an unusual amount of H_2O vapor over the south pole in summer, suggesting that the covering of CO_2 ice had partially disappeared and exposed H_2O ice underneath (*10*). Third, CO_2 ice does not possess sufficient strength (*11*, *12*) to support the 3-km topographic bulge associated with the cap (*13*, *14*) over its inferred lifetime. The implication is that both polar caps are predominantly composed of H_2O ice, although a veneer of CO_2 ice covers the south cap. Here we use the modeling of features seen in imaging data to estimate the thickness of this veneer.

High-resolution imaging from the Mars Orbiter Camera (MOC) (*15*) of the southern residual cap shows quasi-circular depressions (informally named "Swiss cheese features") with flat floors and steeply sided walls [figure 2A in (*16*) and figures 62 through 64 in (*17*)]. Although each feature ranges in diameter from a few hundred meters to more than a kilometer, the depth inferred from shadow measurements is consistent at ~8 m (*16*). The walls show a sequence of layers, with alternating light and dark bands (which may be due to staircase topography) that are each about 1 to

Division of Geological and Planetary Sciences, California Institute of Technology, 1200 East California Boulevard, Pasadena, CA 91125, USA.

*To whom correspondence should be addressed. E-mail: shane@gps.caltech.edu

2 m thick (*16*). Departures from a circular shape tend to line up in the north-south direction, indicating that their evolution is connected with insolation (incident sunlight projected onto the surface). In southern summer ($270° < L_S < 360°$, where L_S is the angular measure of season on Mars), when the seasonally deposited ice has been removed (Fig. 1), the walls of the depressions are darker (*17*) than the flat floors and the surrounding flat upper surfaces (the mesa tops). The walls also expand outward at rates of 1 to 3 m year^{-1} (*18*). This rate of retreat is possible in a volatile medium such as CO_2 ice but not in H_2O ice.

We have developed a model (*19*–*21*) to investigate the growth of circularly symmetric depressions of arbitrary cross section. The shape of the depression evolves as a function of time as CO_2 condenses and sublimes in response to solar and infrared radiation. By assuming circular symmetry, we neglect the slight difference in diurnally averaged insolation between the north and south wall of each depression, provided that they are within a few degrees of the pole. The model (*19*) accounts for incident shortwave radiation (including shadowing), emitted thermal radiation, and all orders of scattered (reflected from point to point within the depression) long- and shortwave radiation. We assign a high albedo (~0.7) to seasonal CO_2 ice that forms and sublimes over the course of each year. The seasonal ice albedo was chosen so that flat surfaces (such as the mesa tops surrounding the depressions) lose as much seasonal ice as they gain and therefore do not change in height from year to year. The temperature of all CO_2 ice within the model is fixed at ~142 K year round by contact with the atmosphere. The H_2O ice may warm up if it is exposed in the summer. This heat is conducted downward and is available to partially offset the condensation of CO_2 during the next winter. Sublimation of H_2O ice is assumed to be negligible on these time scales.

Although we experimented with many model parameters (*22*), only two cases give flat floors, steep sides, and rapidly retreating walls. In both cases, an active slab of CO_2 ice overlies a less active substrate. The active ice slab is composed of dirty CO_2 ice, whose albedo we varied over a range of values but always kept lower than that of seasonal ice. The two possible situations correspond to differing compositions of the less active substrate, which may be either H_2O or clean (albedo of 0.7) CO_2 ice.

Simply inserting an H_2O substrate below a low-albedo slab of CO_2 (Fig. 2A) was partially successful in reproducing the observed depressions. We varied the albedo and thickness of this overlying slab from 0.4 to 0.65 and from 4 to 20 m, respectively. Once the bright seasonal ice is removed, the darker-albedo CO_2 ice is exposed to insolation, causing this initial indentation to grow downward. This growth proceeds until the depression encounters the H_2O ice, after which the floor remains flat from year to year and the walls move outward. In Fig. 2A, the slopes of the walls are ~3°. They will eventually steepen to ~10°, which is less than the typical observed slopes (20° to 40°). In a minority of cases [figure 2C in (*16*)], the observed slopes of the walls of these features are low and match these model results.

To reproduce the higher wall slopes, we allowed the albedo of the dirty CO_2 slab to vary with depth (Fig. 2B). The surface of the mesa top has a high albedo of 0.7; albedo decreases linearly with depth to some minimum value (which we varied from 0.4 to 0.65) at the base of the active slab. The bottom of the active slab receives less sunlight. The lower albedo counteracts this effect and results in a steeper equilibrium slope for the walls. The substrate of H_2O or bright CO_2 ice below the active slab ensures that the floor remains flat. The depression grows down to the substrate, and then the walls expand outward at a constant rate. With an active slab that is 4 m thick, the outward expansion phase begins after ~30 martian years; with an active slab that is 20 m thick, it begins after ~300 martian years. The growth rate is larger when the albedo at the base of the active slab is lower. With the lowest albedo value of 0.4, the growth rate is ~2.5 m year^{-1}; with the lowest albedo value of 0.65, the growth rate is ~0.5 m year^{-1}. These values span the uncertainties in the growth rates (*18*) and albedos measured in the MOC images.

Replacing the H_2O ice substrate with a clean CO_2 substrate produced almost the same morphology and expansion rates (Fig. 2). As with the H_2O ice substrate, the depression first grows down to the substrate and then expands outward. The growth rates depend on the lowest albedo of the overlying dirty CO_2 ice slab as before, although growth rates are slightly larger because of the increased reflected radiation from the bright floor.

To distinguish between an H_2O and CO_2 ice substrate, one needs to observe the temperature of the floors of the depressions. CO_2 ice will always remain at the sublimation temperature because it is in contact with the atmosphere. At the pressures on top of the south polar cap, this temperature is ~142 K. H_2O ice is not subject to this constraint, and when it is exposed in late summer ($310° < L_s < 350°$), its temperature will rise. The maximum brightness temperature occurs at L_s of 320°. We estimate that an infrared instrument such as the Thermal Emission Spectrometer (TES) (*23*) would measure temperatures of 147 and 152 K at L_s of 320°

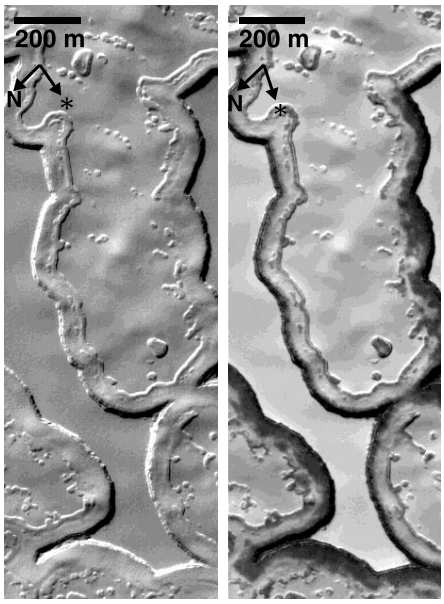

Fig. 1. Changes in albedo when the seasonal CO_2 ice cover is removed and the residual CO_2 cap is exposed. The area shown is at 86°S, 11°E, with subframes of (**left**) M09/04708 and (**right**) M13/02177 at L_s values of 246° and 327°, respectively. Here and in Fig. 3, arrows pointing toward N and * indicate direction toward the north and the Sun, respectively.

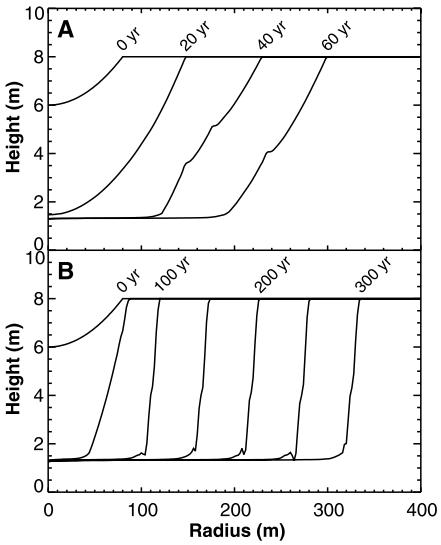

Fig. 2. Model results for a dark residual CO_2 ice slab overlying an H_2O ice base. (**A**) The albedo of the residual CO_2 ice is constant with depth and equal to 0.6. The depression acquires a flat floor, but its walls remain shallow (~3°). (**B**) There is a gradient of albedo in the CO_2 slab from 0.7 at the top to 0.6 at the bottom. The walls develop the characteristic steepness (~30°) of these features and move outward at rates (~1.1 m year^{-1}) consistent with observations.

if the fractions of its field of view occupied by circular depressions were 20 and 40%, respectively. We looked for such signals in the TES data, but effects due to the variable opacity of the atmosphere led to an inconclusive result.

The Thermal Emission Imaging System (THEMIS) on the Mars Odyssey spacecraft (*24*) has a spatial resolution of 100 m and therefore can resolve the larger depressions. THEMIS began taking data after the time of maximum thermal contrast. The earliest available THEMIS image (closest to this time), with a MOC image of the same area, is shown in Fig. 3. The blue (cold) area at the bottom of Fig. 3 (top) is the edge of the residual CO_2 ice cap. The red area is too warm to be CO_2 ice. The MOC image shows that the cold arc in the middle of the warm area is an extended mesa top, with characteristic scalloped sides where the circular depressions have eaten into the walls (Fig. 1). In this place, at least, there is a set of circular depressions whose floors cannot be CO_2 ice, because of their elevated temperatures, and whose mesa tops almost certainly are CO_2 ice. These observations favor the model of a substrate of H_2O ice beneath a thin (~10 m) slab of CO_2 ice. We consider it unlikely that there is a buried CO_2 ice reservoir beneath the H_2O ice, because heat conducted down through the H_2O ice will cause buried CO_2 to sublime (*8*).

The current sizes and expansion rates seem to preclude the initiation of these features being associated with the anomalous 1969 water vapor observation. For features in the region of 350° to 360°E, 86.5°S, our modeling results indicate the year of initiation to be in the range of 1600 to 1920, with the most likely case being ~1900. The spread of ages reflects both the range of current sizes and the range of expansion rates.

The time needed to completely destroy the upper 8-m CO_2 ice slab depends on the spatial density of these depressions and their expansion rate. Taking the region named above as typical, the mean distance between depressions is ~300 m. Two depressions growing toward each other, each at 0.5 to 2.5 m $year^{-1}$, will meet in 60 to 300 martian years and will remove all intervening mesas in 85 to 425 martian years. Large sections of the residual cap appear in MOC images as though the 8-m covering has already been removed. Such areas are probably covered in <2 m of CO_2 ice, which in especially warm years may entirely disappear (as perhaps happened in 1969). The complete history of the residual cap is likely to be much more complicated, with larger (>1 km) features showing signs of multiple initiation events. Although the upper 8-m layer will be removed in a few martian centuries, it is likely that the residual cap has some rejuvenation mechanism and may be in a steady state when its behavior is averaged over time scales of martian millennia.

A central tenet of the Leighton and Murray model (*1*, *8*, *18*) is that the atmospheric CO_2 is buffered by a much larger reservoir of solid CO_2. However, a CO_2 residual ice cap with an area of 88,000 km^2, a thickness of 10 m, and a density of 1.6 g cm^{-3}, would contribute only 0.36 mbar of additional atmospheric pressure if it completely sublimed. This is ~5% of the average surface pressure, so unless there is an additional subsurface reservoir, the Leighton and Murray buffer cannot operate during periods of high obliquity, and the atmospheric CO_2 partial pressure cannot be much larger than its current value. If the CO_2 is mostly in the atmosphere, then the ratio of its mass to the planet's mass is much less than the corresponding ratios for Earth and Venus.

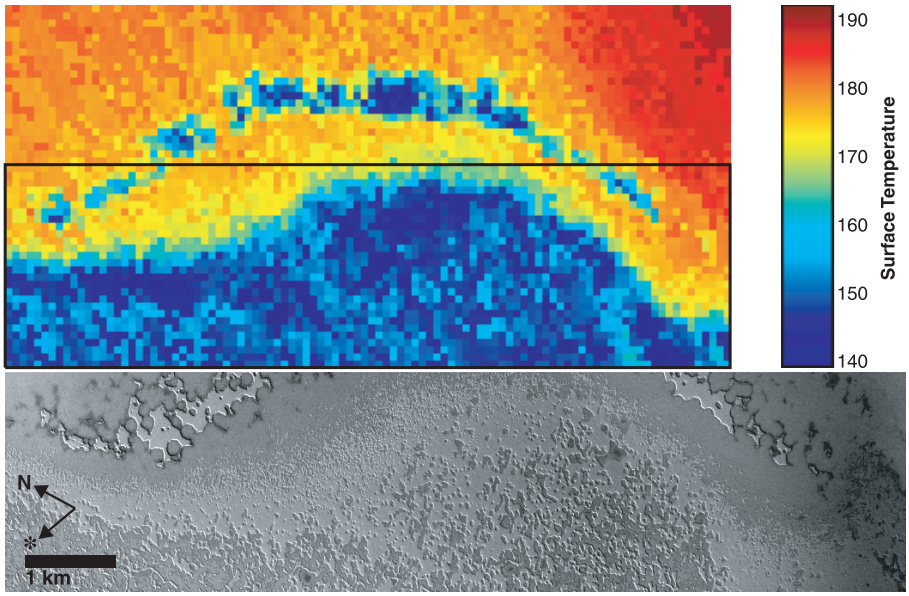

Fig. 3. Example of these circular depressions observed by THEMIS (I00826006) at the cap edge near 84°S, 283°E, at L_s of 330°. (**Top**) Temperatures (in degrees kelvin) derived from THEMIS radiance measurements in an area that is 10 km by 5 km. The boxed area corresponds to (**bottom**) the subframe of MOC narrow-angle image M03/04994. Cold (blue) material corresponds to the CO_2 mesa tops, and warm (red) material corresponds to terrain surrounding the mesas and making up the floors of the depressions. These data rule out clean CO_2 ice as the substrate in this area.

References and Notes

1. R. B. Leighton, B. C. Murray, *Science* **153**, 136 (1966).
2. B. C. Murray, M. C. Malin, *Science* **182**, 437 (1973).
3. H. H. Kieffer, *J. Geophys. Res.* **84**, 8263 (1979).
4. _____, S. C. Chase, T. Z. Martin, E. D. Miner, F. D. Palluconi, *Science* **194**, 1341 (1976).
5. C. B. Farmer, D. W. Davies, D. D. LaPorte, *Science* **194**, 1339 (1976).
6. P. B. James, H. H. Kieffer, D. A. Paige, in *Mars*, H. H. Kieffer *et al.*, Eds. (Univ. of Arizona Press, Tucson, AZ, 1992), pp. 934–968.
7. P. C. Thomas, S. W. Squyres, K. E. Herkenhoff, A. Howard, B. C. Murray, in *Mars*, H. H. Kieffer *et al.*, Eds. (Univ. of Arizona Press, Tucson, AZ, 1992), pp. 767–795.
8. A. P. Ingersoll, *J. Geophys. Res.* **79**, 3403 (1974).
9. S. E. Wood, D. A. Paige, *Icarus* **99**, 1 (1992).
10. E. S. Barker, R. A. Schorn, A. Woszczyk, R. G. Tull, S. J. Little, *Science* **170**, 1308 (1970).
11. W. B. Durham, S. H. Kirby, L. A. Stern, *Geophys. Res. Lett.* **26**, 3493 (1999).
12. J. F. Nye, W. B. Durham, P. M. Schenk, J. M. Moore, *Icarus* **144**, 449 (2000).
13. D. E. Smith *et al.*, *Science* **284**, 1495 (1999).
14. P. M. Schenk, J. M. Moore, *J. Geophys. Res.* **105**, 24529 (2000).
15. M. C. Malin *et al.*, *J. Geophys. Res.* **97**, 7699 (1992).
16. P. C. Thomas *et al.*, *Nature* **404**, 161 (2000).
17. M. C. Malin, K. S. Edgett, *J. Geophys. Res.* **106**, 23429 (2001).
18. M. C. Malin, M. A. Caplinger, S. D. Davis, *Science* **294**, 2146 (2001).
19. We used a matrix inversion approach ("radiosity") to calculate all orders of scattering. By assuming circular symmetry, we only have to keep track of annular bands. All surfaces are assumed to be Lambert scatterers. The time step is 1° of L_s, which is ~2 days. We verified the model against the analytic solution for spherical bowl-shaped craters.
20. A. R. Vasavada, D. A. Paige, S. E. Wood, *Icarus* **141**, 179 (1999).
21. A. P. Ingersoll, T. Svitek, B. C. Murray, *Icarus* **100**, 40 (1992).
22. We experimented with depressions embedded in pure (clean at all depths) CO_2 ice and found them to be self-erasing. Depressions in dirty CO_2 ice with no resistant substrate grew indefinitely as shallow bowls, which are not observed on the residual cap. Initial size and shape had no effect on long-term behavior in all cases. Albedo and thickness of the dirty CO_2 ice slab ranged from 0.4 to 0.65 and from 4 to 20 m, respectively. H_2O ice albedos were set to the same value as those of the CO_2 directly above it (that is, the bottom of the dirty slab).
23. P. R. Christensen *et al.*, *J. Geophys. Res.* **97**, 7719, (1992).
24. P. R. Christensen *et al.*, in preparation.

25. We thank O. Aharonson, A. Albee, B. Murray, N. Schorghofer, and two anonymous reviewers for helpful comments and NASA's Mars Data Analysis Program and Mars Global Surveyor project for financial support.

5 November 2002; accepted 23 December 2002